Elucidation of the origins of transport behaviour and quantum oscillations in high temperature superconducting cuprates

2009 J. Phys.: Condens. Matter 21 245702

(http://iopscience.iop.org/0953-8984/21/24/245702)

J. Phys.: Condens. Matter **21** (2009) 245702 (16pp) doi:10.1088/0953-8984/21/24/245702

Elucidation of the origins of transport behaviour and quantum oscillations in high temperature superconducting cuprates

John A Wilson

H H Wills Physics Laboratory, University of Bristol, Tyndall Avenue, Bristol BS8 1TL, UK

E-mail: john.a.wilson@bris.ac.uk

Received 19 November 2008, in final form 22 April 2009
Published 26 May 2009
Online at stacks.iop.org/JPhysCM/21/245702

Abstract

A detailed exposition is given of recent transport and 'quantum oscillation' results from high temperature superconducting (HTSC) systems covering the full carrier range from overdoped to underdoped material. This now very extensive and high quality data set is here interpreted within the framework developed by the author of local pairs and boson–fermion resonance, arising in the context of negative-U behaviour within an inhomogeneous electronic environment. The strong inhomogeneity comes with the mixed-valence condition of these materials, which when underdoped lie in close proximity to the Mott–Anderson transition. The observed intense scattering is presented as resulting from pair formation and from electron–boson collisions in the resonant crossover circumstance. The high level of scattering carries the systems to incoherence in the pseudogapped state, $p < p_c$ (=0.183). In a high magnetic field the striped partition of the inhomogeneous charge distribution becomes much strengthened and regularized. Magnetization and resistance oscillations, of period dictated by the favoured positioning of the fluxon array within the *real space* environment of the diagonal 2D charge striping array, are demonstrated to be responsible for the recently reported behaviour hitherto widely attributed to the quantum oscillation response of a much more standard Fermi liquid condition. A detailed analysis embracing all the experimental data serves to reveal that in the given conditions of very high field, low temperature, 2D-striped, underdoped, d-wave superconducting, HTSC material the flux quantum becomes doubled to h/e.

1. Background to negative-U modelling of HTSC phenomena

It long has been realized that the normal state properties of HTSC cuprates, whether electrical, magnetic or optical, are highly unusual, and bear an intimation of what is to follow within the low temperature superconducting condition [1]. All the normal state properties give indication of chronic electronic scattering, especially along the axial Cu–O planar bond direction; i.e. in the antinodal direction of the superconductive d-wave state and containing the saddle points of the Fermi surface and their so-called 'hot spots' (the latter associated with the oblique diagonals of the BZ quadrants; see figure 3 in [2]). This unusual scattering becomes increasingly manifest as the employed 'doping' level is lowered through the overdoped condition towards p^{opt}, and to it is attributed the steady rise with cooling in the magnitude of the observed p-type Seebeck [3, 4] and Hall [5] coefficients toward non-metallic levels.

ARPES was the first technique to reveal directly that this scattering-induced degradation in Fermi behaviour sets in from the zone-edge saddles and slowly develops round the Fermi surface (FS) in the direction of the 45° zone diagonals as both p and T fall [6, 7]. This impairment of band-like quality (i.e. induced incoherence) that the carriers undergo with decreasing hole 'doping' does not initially see a diminution in $T_c(p)$ but, rather, an increase. However, as long known from electronic specific heat studies [8], somewhat in advance of reaching $p(T_c^{max})$ the superconducting condensation energy suddenly collapses. From my long-

standing perception of HTSC phenomena as being the outcome of a resonant boson–fermion crossover in an inhomogeneous (mixed-valence) negative-U setting [1, 9], this collapse is taken to be the moment FS disintegration finds coherent quasiparticle status extinguished at the hot spots. (The latter are the k-points from which the doubly-loaded negative-U states ($^{10}Cu^{2-}_{III}$) are most favourably accessed [2].) There then ensues a rapid development and extension in the density-of-states 'pseudogap' to lower p.

In real space I have indicated in figure 5 of [10], within the dynamic stripe phase context of LSCO, that the moment at which maximum condensation energy arrives bears very close association with a $7 \times 7a_o$ 'stripe' structure and doping content $p = 0.183$. At this stage as the key carriers are driven close to their band-like limit they are rendered best able to form and support long-lived local pairs within the Cu_{III} clusters of site-charging which the 2D striping geometry presents. A 7×7 structure is, note, spatially compatible with the given hotspot location. Mention of Cu_{III} clusters emphasizes here that the negative-U state is associated not with the copper cations *per se*, but with entire Cu–O coordination units. The key to the negative-U effect is the p^6d^{10} shell closure achieved upon the Cu_{III} site charge double-loading $^{10}Cu^{2-}_{III}$ and the ensuing total reordering of the till now strongly $\sigma\sigma^*$ bonding and antibonding O(p)/Cu(d) states [9].

The local pair states being so generated are most effective at elevating T_c when they are neither too localized (or few in content) as at low p, nor are too short-lived and weakly interactive as under the well-screened conditions of high doping. In the desired crossover conditions of the fermion–boson mix, the local pair bosons need to uphold within the Fermi sea as many ancillary BCS-like quasiparticle couplings as possible. The optimal of optimum conditions at raising T_c^{max} is acquired by selecting that material for which the negative-U state binding energy ($\mathcal{U}$) below E_F stands resonant with the induced chemical potential at the very moment set by the geometrical condition above and the completion of the DOS pseudogapping at the hot spot. Control in achieving these optimized circumstances is granted within the present scheme by a manipulation of the ionicity of the counter-ions incorporated into the system. $HgBa_2Ca_2Cu_3O_{16+\delta}$ currently constitutes the most favourable combination. What the selected level of covalency of the overall system permits is close control over the metallic screening operative within the material and of the dielectric constant to follow. If a system is too covalent (as say $Bi_2Sr_2CuO_{6+\delta}$), metallic screening remains too active at $p = 0.18$ and the population/life-time of the local pairs becomes diminished. If the system is too ionic (as say $(Na_xCa_{2-x})CuO_2Cl_2$) then by $p = 0.18(\downarrow)$ the quasiparticle incoherence will have become too advanced and the number of induced BCS-like pairs that can be sustained reduced. Note a small degree of gain in stability for the local pairs can be tolerated at the expense of some minor loss in band carrier number. Indeed T_c^{opt} uniformly is to be found at $p = 0.16$ not 0.18, but equally uniformly remember that the superconductive condensation energy per Cu atom maximizes at the latter concentration within all cuprate HTSC systems [8].

The systematics of the connection between the final (d-wave) superconductive gapping parameter Δ_o^{max} and $\mathcal{U}$, the negative-U state binding energy, when arrayed as functions of doping and system covalency has been sketched out in figure 4 of [11] using information drawn in the main from energy- and position-resolved scanning tunnelling microscopy, from ARPES and from neutron scattering. The scheme presented in [11] has very recently received added support from the p-dependent STM results for Bi-2212 just published by Kohsaka *et al* [12]. Needless here to say, there is continued strong departure in the interpretation which the latter team offer of their results, although it is good to see now the nodal/antinodal dichotomy being acknowledged in relation to the two principal energies involved in the phenomena. (Beware when comparing figure 3b in [12] with my figure 4 in [11] that in the former the modes plotted for the four different p values have received increasing zero offsets.) Kohsaka *et al* are unable to perceive why the features they record exist only over a limited range of angles ϕ around the Fermi circle. Within my understanding that arises because the mode in question, the dispersed uncondensed pair mode [9c], is defined sharply only between the hot spots and where this linearly dispersed mode emerges above E_F. Note while the induced nodal superconductivity is demonstrably of $d_{x2-y2}B_{1g}$ symmetry, the local pair state takes angularly empathetic but distinct, extended-s, A_{1g} form. The local pairs become unstable near the zone centre, and in truth in the STM data there occurs no indication that the observed modal feature pulls round in simple d_{x2-y2} fashion toward the gap node. Note all recorded very low energy investigations in HTSC materials, such as electronic specific heat, penetration depth, B_{2g} electronic Raman and optical measurement, are ones concerning the induced BCS-like pairing.

Section 2 below tracks in detail the development of the abnormal electrical and optical properties of HTSC systems as 'hole doping' is reduced below $p = 0.3$. For the latter the position of the Landau Fermi liquid behaviour is fairly standard if highly correlated. Below $p = 0.3$ there arises marked growth in scattering and a steady shift towards incoherence. Apportionment of the unusually strong scattering into elastic and inelastic, isotropic and anisotropic contributions is presented in terms of e/e-to-b and e-on-b events from a close examination of the T- and p-dependent evolution of the AMRO, Seebeck and Hall data.

Section 3 takes a detailed look at the new high quality $\rho(T, p)$ resistivity data and analysis from LSCO, and at the changes suddenly occurring at $p = p_c(=0.18)$. The nature of what arises there as one encounters strong incoherence and the pseudogap condition is fully described in terms of the crossover model.

Section 4 follows up on the consequences of such an interpretation and attempts to reformulate the setting of the high field oscillatory magnetization, resistivity and Hall data recently obtained from UD material in terms *not* of a standard quantum oscillation, k-space response of a fairly normal Fermi liquid, but of real-space-based action much more appropriate to the UD condition. Success here is demonstrated to revolve around the 2D striping supported by such mixed-valence materials, and seemingly enhanced in definition by the strong applied magnetic field. The model is one of response to the free energy changes arising as the unpinned vortex array slips

discretely past the doping determined stripe array. A very close match to the experimental data can be secured *provided* that the flux quantum in question in this ring-threading process is not $h/2e$ but h/e. The observations are related back to Forgan and colleagues' SANS observations on UD material of a transfer from hexagonal to square symmetry in the vortex array geometry as the magnetic field is increased.

2. The nature of the scattering governing HTSC transport and optical behaviour

Following this introduction I wish now to examine in detail the important recent work from my colleagues in Bristol relating to such matters, work in the main performed under strong magnetic fields in excess of 30 T. Their dc and ac resistivity data [13, 14], their Hall data [15], and their now renowned Fermi surface quantum oscillation data [16–18] all afford great potential insight into the above matters. Unfortunately it must be said that it has not proved possible to get them as yet to commit themselves with regard to the HTSC mechanism. As I have long since jumped, it is incumbent upon me here to offer interpretation along the above lines of the phenomena they are reporting. In this it is best to proceed following roughly the order in which the data were acquired, starting with the AMRO (angular magneto-resistance oscillation) results on overdoped $Tl_2Ba_2CuO_{6+\delta}$ (Tl-2201) [16].

Tl-2201 is a very valuable system within the array of HTSC materials in that it is structurally simple (bar some cation cross-substitution), is of relatively high T_c^{max} (∼95 K), and, above all, it may be taken from optimal hole doping right through into the range beyond $p = 0.28$ where superconductivity has vanished. On dropping to somewhat smaller p than this, one is able to stay within the normal state and study the low temperature condition there upon the application of magnetic fields in excess of $H_{c2}(p, T)$. Under these conditions the AMRO work delivered the first low energy, low temperature record of a relatively well-formed Fermi surface in highly overdoped material. Of course, as the level of p doping is reduced, T_c quickly picks up and $H_{c2}(p)$ passes above 50 T, thereby limiting further investigation. However it was very apparent even from the limited range accessed that scattering in the system is mounting rapidly as p is reduced, bringing down the $\omega\tau_c$ values extracted from the data to below unity. The most significant observation made in the analysis of this AMRO work was that the abnormal intense scattering is comprised of an elastic, anisotropic ($\propto v_F^{-1}$), temperature-independent base term and two temperature-dependent terms, one characterized by T-linear behaviour and strongly anisotropic in form (this, like the base term, maximal in the axial saddles) and the other term (comparatively) isotropic but inelastic and characterized by a T^2 variation.

$$\Gamma(T,\phi) = \{\Gamma_0(\phi) + \Gamma_1 \cos^2(2\phi)T\} + \Gamma_2 T^2$$

	anisotropic		isotropic
	elastic	inelastic	inelastic
—ascription made in present text:		electron–boson	electron–electron to boson.

These temperature behaviours extend up to such values as affirm their sourcing to be purely electronic and not phononic. Normally T^2 e–e Baber scattering is in evidence only at very low temperatures, prior to it being swamped by e–ph scattering, but clearly the e–e scattering now in play must be super-effective for the term to remain in evidence at all temperatures. In [1, 19] it was submitted that such a T^2 term must represent local pair boson formation. It comes to dominate nodal scattering. How long the pairs persist will depend upon the p-value and the level of screening supported (although not overly upon the temperature once above T_c, as is apparent from laser pump–probe work [19]). Naturally when screening falls as p is reduced, these bosons acquire a longer life-time and the population of pairs, both local and induced, mounts steadily as p drops towards p^{opt} at 0.16/0.18. By that stage one can anticipate e–b scattering is going to predominate, the T^2-term to the strong scattering now yielding primacy to the T-term.

The e–e → b isotropic scattering in its strongly inelastic character reflects its third party nature, the lattice needing locally to accommodate (swell) under the Cu_{III} site, charge double-loading event. Inevitably here within a highly correlated system the electrons cannot be treated in isolation from the lattice, as is made very apparent from the isotope effect data [20], the neutron-acquired soft mode data [21], the reported transient laser-induced changes in lattice parameter [22], and indeed from direct lattice and bond length measurements themselves [23, 24]. In contrast to the above, once the population of axially stabilized bosons is extensively acquired, under such p levels as to support T_c^{max} and E_{cond}^{max}, the then dominant e–b scattering is anisotropic and quasi-elastic. Each scattering boson naturally is here unrestricted by the Fermi principle in regard to the k-states into which it is able to pass. Hence whilst this electron-on-boson scattering is very intense because of the augmented scattering cross-section, it predominantly will be small angle in form. As was previously expressed in [9b], the source suggested by Varma and Abrahams [25] for this small angle scattering in HTSC materials is not seen as being realistic; namely scattering off the 'defects', intrinsic and otherwise, residing between the CuO_2 layers. Why then (i) the observed very strong thermal augmentation; (ii) its occurrence in OP Y-123 and in lattice perfect Y-124; (iii) its super-strong showing exclusively for HTSC materials and relative absence for partially intercalated layer compounds such as Na_xTiO_2 or Cu_xTiS_2? The current scattering, as expounded upon recently by Zaanen [26], is taking the HTSC materials to the verge of incoherence, with $h/\tau \to 2\pi kT$. It is occurring, what is more, in materials that, as a result of the advanced p–d mixing in hole-doped cuprates, display a mean-field LDA bandwidth for the FS-containing d_{x2-y2} sub-band manifesting the not insubstantial value of 2 eV plus [27].

Everything recorded about HTSC materials implies marginal Fermi liquid (MFL) behaviour of some form [25]. Hence one is obliged not to allow the recent observation of dHvA oscillations in very strongly overdoped Tl-2201 [13] to obscure this basic aspect once one enters the HTSC range of p. In particular this becomes the case for underdoped Y-123 and Y-124 in regard to the purported revelation of small, rather ordinary FS pockets from SdH and similar experimentation [18]—of this much more later. HTSC

materials are far from being ordinary metals as any glance at the low temperature infra-red results will reveal (with their sizeable mid-IR oscillator term, residual temperature-dependent Drude term, and scattering $h/\tau \sim 2\pi k_B T$) [28]. Even ignoring matters specifically involving the l.t. condition, the proximity of the cuprates to Mott insulation (extant in *all single*-valent Cu_{II} and Cu_{III} oxides) plus the strong local disorder, electronic as structural, implicit with the mixed-valence of the HTSC cuprates, ought immediately to direct one away from simplistic considerations of what is afoot. Nowhere is that more in evidence than when confronting Hall data for the HTSC materials. Although the (300 K) Hall constant sign is positive, as might well emerge from a Fermi surface centred upon the zone corner, its magnitude is remarkably high at low substitution levels away from band half-filling, a fact that has greatly contributed with the HTSC cuprates to the whole notion and terminology of 'hole doping' p away from the d_{x2-y2}-based Mott state, $^9Cu^0_{II}$. The task set is to tread warily through the complex region between band and localized behaviour without any lapses of concentration, such as those perceived to have arisen in much discussion of the recent SdH/dHvA work on underdoped material ($p \sim \frac{1}{8} - \frac{1}{10}$). The low energy Hall [5, 15] and Seebeck [3, 4] data afford the most favourable point of entry to penetrating this crossover behaviour.

One of the early-noted empirical rules established by Obertelli *et al* [4] was that in every HTSC system the Seebeck coefficient for optimally doped material always on warming changes sign from positive to negative at just about 300 K. The early ad hoc analyses of this temperature-dependent Seebeck coefficient invariably revolved around standard gaps. The latter were universally determined as being extremely small (<50 meV), and in [3b] it was indicated that this was not an appropriate model with which to proceed. Informed by the early electronic specific heat analysis from Loram *et al* [8] and the formal treatment of the Seebeck coefficient provided by Hildebrand *et al* [29], we in [3a] presented a treatment of such data from Hg-1201 based upon a negative-U approach with density of states pseudogapping in the presence of resonant BF scattering. In the thermoelectric expressions the observed positive sign of S is introduced by the sign at E_F of the gradient $\partial\sigma/\partial E$ being negative, which in turn issues from $\partial\tau/\partial E$ and/or $\partial n_{\rm eff}/\partial E$ being negative. In optimally doped systems such a state of affairs terminates by 300 K, but with underdoped systems the pseudogapping onset temperature continues to mount, a feature now well-monitored in STM and ARPES work, and the Seebeck coefficient stays positive to raised T. Note this many-body pseudogap condition becomes lost towards T^* not via reduction in gap energy but via DOS 'in-fill'—hence its name.

With the Hall coefficient the analysis of the conversion from positive to negative sign is not quite so straightforward, and crossover does not occur at the same $\{p, T\}$ combination as for the Seebeck coefficient. This is because the Hall process is a transverse one, it, as was demonstrated by Ong [30], being dependent upon the cross-product, Stokes area integral in k-space at $E_F - \int_{FS} d\boldsymbol{\ell} \times \boldsymbol{\ell}$ relating to the local mean free path vector $\boldsymbol{\ell}$ at each particular $\mathbf{k}_F$. The different weightings within the integral coming from different bits of Fermi surface are, in addition to anisotropy in $\mathbf{v}_F$, thus dependent upon the anisotropy of the scattering rate $1/\tau(\mathbf{k}_F)$ (i.e. on that of $\boldsymbol{\ell}(\mathbf{k}_F)$), and this critically so when that scattering is super-strong and highly anisotropic as in the present case. The outcome is that, for many HTSC materials, R_H remains positive to very high temperatures and also to surprisingly high p values—indeed even to beyond where in LSCO the band saddle-point has been surmounted and the FS become closed about the zone centre rather than the zone corner.

Figure 1 illustrates the latter circumstance for OD-LSCO, drawn appropriate to the level of anisotropy in $\boldsymbol{\ell}(\mathbf{k}_F)$ disclosed by the AMRO work on OD TBCO, following analytical treatment which, as long as coherence is fully maintained, remains able to assume standard Boltzmann–Zener–Jones-type form. Out at $p = 0.3$ we are looking at strong anisotropy in basal $\mathbf{v_F}$ of about 3.5, but for $|\boldsymbol{\ell}|$ (or scattering rate $1/\tau$) only a weak anisotropy at 300 K of about 10% remains. As p and particularly T are reduced the evaluated anisotropic (e-on-b) contribution to $1/\tau$ steadily mounts. Ultimately there has to come an end to the validity of the BZJ analysis somewhere in advance of $p = 0.183$, the value signalled above as marking the quasiparticle coherence limit at the hot spots. Nevertheless the modelling presented in figures 3 and 4 of [15] by Narduzzo *et al* of the rising magnitude of R_H under falling p and T was quite promising. In fact at the time only the T^2 term and the band anisotropy in $\mathbf{v}_F$ were inserted into the analysis, suspecting Fermi liquidology to prevail. The outcome clearly was, though, to understate the rise in R_H as p dropped. What could not, moreover, be captured was the growth upon cooling, as the local pairs move into operation, of actual precursor superconductivity within micro-regions where $\sigma \to \infty$ (i.e. $V_{RH} \to 0$). From low field work one notices well in advance of T_c itself that the Hall coefficient, as with the Seebeck coefficient, begins to disclose its compulsory decline towards zero at T_c, this turn about being encountered the earlier the more underdoped a sample is, i.e. the greater $\mathcal{U}$ and T^* there. Such behaviour parallels what is in evidence in the Nernst data above T_c [31, 9c].

To secure a truly satisfactory outcome to all these scattering calculations, whether when handling under- or overdoped HTSC data, Hussey *et al* [32] demonstrated some time ago that it is necessary to supplement application of the scattering equation above somewhat further. In consequence of the strongly temperature-dependent terms there, the average scattering mean free path quickly is reduced to approach the Mott–Ioffe–Regel limit of $\boldsymbol{\ell} \approx a$ (the lattice parameter). This marks the coherence limit to band-like quasiparticle behaviour ($\mu \sim 1$ cm^2 V^{-1} s^{-1}). It affords a ceiling within many heavy scattering materials, such as the A15's, against unending escalation in the overall scattering rate, in what has become known as 'resistance saturation' [33]. When scattering is highly anisotropic the approach to saturation inevitably will reflect the strongly directional nature of $|\boldsymbol{\ell}(\mathbf{k}_F)|$ around the Fermi surface. The situation calls for an added resistance-limiting term to obtain what rather unfortunately has become known as the 'parallel resistance' formulation. In this the effective net scattering rate $\Gamma_{\rm effective}$ ($\propto 1/\boldsymbol{\ell}_{\rm eff}$) is secured from the original expression $\Gamma_{\rm ideal}$, via the inclusion of a saturation

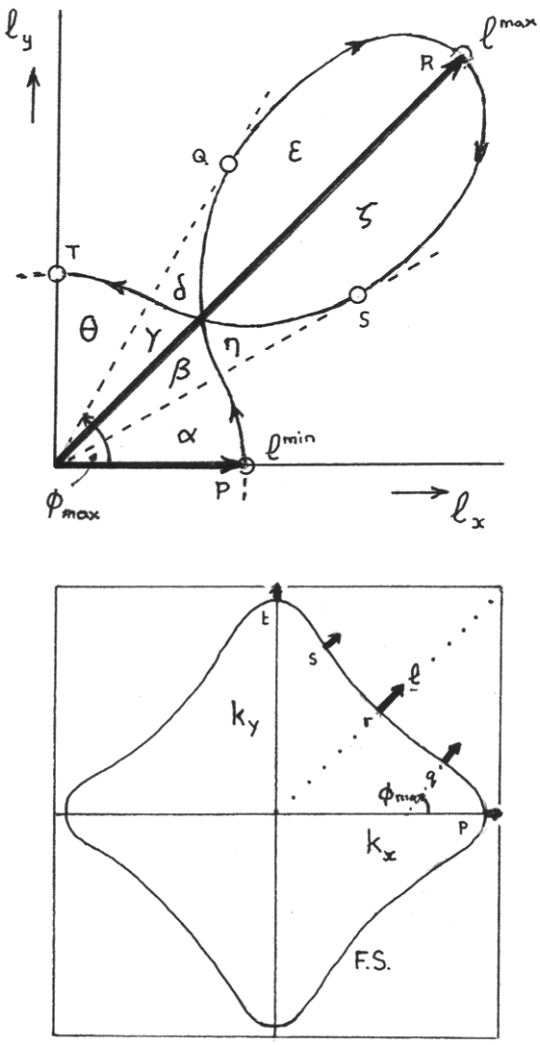

Figure 1. Schematic rendering of the way in which the strong anisotropy existing in the mean free path $\boldsymbol{\ell}(\mathbf{k}_F)$ controls the magnitude and sign of the Hall coefficient in overdoped HTSC materials. The latter sign is dictated by the Ong integral $-\int_{FS} d\boldsymbol{\ell} \times \boldsymbol{\ell}$ taken around the Fermi surface [30]. The signs of the incremental contributions are here set by the sense locally of the circulation of the cross-product; counter-clockwise circulation leads to negative contributions to R_H, clockwise to positive. The construction shows how the net sign of the integral depends on the difference in area of the two types of closed segment generated within the full circuit traced out by $\boldsymbol{\ell}(\mathbf{k}_F)$. The figure is produced for the situation appropriate to OD-LSCO, which has the form of FS indicated and where a small mean free path in the axial directions converts to a much larger mean free path in the diagonal 45° directions. The outcome is a positive Hall coefficient in spite of the Fermi surface here being closed about the centre of the BZ, not the corner. The special locations for $\boldsymbol{\ell}(\mathbf{k}_F)$ marked P to T divide the $\boldsymbol{\ell}(\mathbf{k}_F)$ picture up into areas designated α to θ (and match points p to t for $\mathbf{k}_F$ around the Fermi surface). q is the point of curvature inflection on the FS and tangential point Q on $\boldsymbol{\ell}(\mathbf{k}_F)$ marks the associated maximum to angle ϕ for points within the first half-quadrant. Signs are inserted both by $d\boldsymbol{\ell}$ and by the vector cross-product. Where $d\boldsymbol{\ell} \times \boldsymbol{\ell}$ is positive from P to Q, the integral itself is given by $+(\alpha + \beta + \gamma + \delta)$, where $d\boldsymbol{\ell} \times \boldsymbol{\ell}$ is negative from Q to S, the integral itself is given by $-(\gamma + \delta + \varepsilon) - (\beta + \eta + \zeta)$, where $d\boldsymbol{\ell} \times \boldsymbol{\ell}$ is positive from S to T, the integral itself is given by $+(\beta + \eta + \gamma + \theta)$. So for entire repeating quadrant the net the integral itself is given by $+(\alpha + \beta + \gamma + \theta) - (\varepsilon + \zeta)$,—or taken over all four quadrants, the difference in areas of the counter-clockwise minus clockwise enclosed areal segments—and here negative, making R_H positive.

scattering term $\Gamma_{maximum}$ such that $1/\rho_{eff} = 1/\rho_{ideal} + 1/\rho_{max}$: the terminology employed by Hussey in [32] is used here. The expression effectively is one of conductances acting in sequence and it relates to coherent and incoherent micro-segments within the overall transport process. In order to control the number of free parameters in the numerical work, the angular and p dependence of ρ_{max} have customarily been suppressed, a universal value being inserted for ρ_{max} of nearly 1 mΩ cm ($\equiv h\Gamma_{max} \sim 3000\ \mathrm{cm}^{-1}$ or 0.4 eV). Despite complete saturation in OD-Tl-2201 not being encountered until 600 K, this extra term is found to make its presence felt at much lower temperatures.

As states become incoherent (i.e. lose their band-like quality) they will relinquish any related p-type signing in regard to the contribution which they make to the Hall coefficient (although note amorphous and glassy metals can be p-type [34]). Prior to actually being lost to the band-like cohort the near-axially directed quasiparticles are of very low mobility and despite being great in number the contribution which they make here to R_H is not dominant. Recall in Hall work the quantity the Hall mobility, $\mu_H = R_H H_z/\rho$, often is introduced. In the present case μ_H is going to be dominated by those carriers moving in the less severely scattered nodal directions. Such carriers are suffering in the main just the (isotropic) e–e → b based scattering, T^2 in form. Accordingly μ_H, or its equivalent $\tan\theta_H/H_z$, will overall be proportional to T^{-2} [1]. Indeed the empirical relation $\cot\theta_H = A + BT^2$ long has constituted one of the best recognized elements of HTSC phenomenology [35]. We see now this ubiquitous (approximate) form occurs by virtue of the very strongly anisotropic nature to the electron–boson scattering, high in the saddles and low in the nodal directions. Within the diagonal stripe modelling of [10] note, in addition, that the nodal direction provides the easy 'rivers of charge' direction. It may well be that the T^2 scattering term actually develops some anisotropy of its own as p and T fall, but carrying this contrasting B_{2g} geometry to the B_{1g} form of the T term.

For those who have not yet adjusted to 'nodal rivers of charge', it is suggested they look again at the outcome of Homes *et al*'s sub-60 K infra-red study on $p = \frac{1}{8}$ LBCO (wherein T_c is much depressed) [28b]. At such T and p many carriers, as manifest from the dip in the IR reflectance edge, have become rendered incoherent and ineffective at contributing towards the Drude optical response. As *axially* oriented carriers become incoherent, those quasiparticles left in the nodal direction actually become less strongly scattered and the residual Drude peak indeed sharpens up at the lowest temperatures. Such carriers running freely in the nodal directions, and maintaining the Fermi arc signal of ARPES work [6], express a 2D behaviour completely at odds with the much advocated 1D setting to stripe formation and activity (see [10]). Not only does the T^2 scattering behaviour characterize the nodal response, but it is echoed too optically in a nodal self-energy that varies as ω^2 [36]. Aeppli *et al* [37] many years ago in fact observed that the high energy, inelastic neutron scattering π, π 'resonance' linewidth exhibits a joint dependency upon ω and T proceeding as $\sqrt{(\omega^2 + T^2)}$. To close this section note that in LBCO under the above conditions the

Hall coefficient is not actually positive but negative [18c, 18d], a matter of some import to which we shall return.

Let us before that turn again to the Bristol-based transport work of Hussey and colleagues. Whilst Hussey proceeds in his review of [32b] to deal next with the very unusual magneto-resistance data over the matter of their non-Kohler-like behaviour, we, within the framework already developed, are in a position now to address directly their most recent high field resistance results from high quality, single crystal samples of optimally and overdoped LSCO [13]. This new data stands sufficiently accurate and self-consistent between the different samples to allow a really close investigation into how the scattering progresses with reduction in T and p. The new paper has been couched actually within the presently popular setting of quantum critical phenomena, but the outcome is far from what some had anticipated, and it affords a most revealing view of what really is underway within HTSC materials.

3. Detailed look at new resistivity and Hall data in relation to HTSC mechanism

The new data [13] come from a sequence of eight different, well-specified compositions of LSCO single crystal with p running from 0.17 to 0.33, and were acquired under z-axis magnetic fields of up to 60 T. The quality of the data is such as to make it possible meaningfully to fit to the full scattering procedure above and to extract the p-dependent behaviour for coefficients α_1 and α_2 relating respectively to the T and T^2 terms. This requires being able satisfactorily to extrapolate the observed $\rho(H, T, p)$ plots down into the superconducting regime below the relevant $H_c(T, p')$ values so as to uncover the l.t. condition which would prevail in the absence of LRO superconductivity. The extrapolation too has to traverse appropriately the SRO fluctuation range above H_c and/or T_c. What is found is that right up to $p = 0.33$ *both* T and T^2 terms always are present, but that their relative weighting changes most illuminatingly both with regard to p and T.

As indicated above some among the authors of the work had expected to be able to link their findings into the general discussion on quantum critical phenomena, after the fashion of various rare-earth systems. There a linear-in-T behaviour for ρ is associated with a rather narrowly divergent fan on the T versus x (or P) phase diagram, flanked by T^2 Fermi liquid behaviour. However, one observes for the HTSC system that in fact both terms run concurrently throughout the entire superconducting range of p, and, moreover, that the (anisotropic) linear-in-T term, instead of fanning out to high T, is dominant at those low temperatures for which pairs are to be found, i.e. onsetting around T^* and particularly below T_c. As claimed earlier this linear contribution is surely the expression of e-on-b scattering. If one proceeds with a single-term empiric formulation $\rho \propto T^n$, as often has been adopted in the past, then exponent n drifts from 2 towards 1 as T and p fall and the life-time and instantaneous population of bosons build.

Interestingly the analysis, as conducted in [13], does not manage to pick up any augmentation in e–e $\rightarrow$ b pair production success with fall either in T or p (as gauged by the discerned behaviour of α_2 for the T^2 term). There occurs no detectable change in coefficient α_2 right from $p = 0.33$ down to p_c. By contrast the evaluated α_1 (e-on-b) coefficient augments steadily with reduction in T or p, as the population of bosons mounts. Once again the latter behaviour continues through until p falls to p_c. So what is this p_c? It is 0.183, the value of doping for which the superconducting condensation energy per carrier is at a maximum [10], as revealed by the specific heat analysis of Loram *et al* [8]. The combination of boson population and boson binding energy has become optimized at this juncture. As stated already, it is with this concentration one seriously is encountering incoherence in the quasiparticle system. Below this hole concentration quasiparticles rapidly become abstracted from the coherent response of the system and the condensation energy falls away sharply. While the Uemura plot, made from muon penetration depth work [38], had revealed from low p the steady build up in pair numbers n_s, the effectiveness of those pairs in advancing the global condensation energy was, it is evident, somewhat less than their effectiveness at raising T_c. From p_c down into the sub-optimally doped region, where the local pairs are dropping out of resonance with E_F, the energetics of the coupling between the two subsystems, their fermions and bosons, is declining [11], and at low p ρ returns to being dominantly quadratic in form [39].

So how is this manifest in the new resistivity results as one proceeds below p_c? α_1, having come to a broad peak at p_c, now falls away quite steeply. Conversely α_2, so long p-independent, exhibits a sharp upward movement below p_c, bringing a higher absolute and relative contribution to ρ. By T_c ($\approx$33 K) the magnitude of α_1 at p_c is driving the value of ρ to its coherence limit of 1 mΩ cm. As expressed previously, the downturn in α_1 below p_c declares a drop-off in the overall boson population, if the linear-in-T term indeed is registering e–b scattering activity. p_c stands at the tip of the Uemura 'butterfly wing', i.e. of the $T_c(p)$ versus $n_s(p)$ plot [38]. Conversely with e–e $\rightarrow$ b scattering indeed assayed by the T^2 term, α_2s sudden rise below p_c (for all T) must express the enhanced cross-section towards local pair production once metallic screening starts to collapse with the onset of large-scale quasiparticle incoherence. As noted by Hussey and co-workers [13] this counter-movement between α_1 and α_2 met with at p_c is the precise opposite of what might have been expected were one looking at standard quantum critical behaviour. This truly is new physics—but not that physics.

The development of incoherent quasiparticle behaviour below p_c is immediately picked up also in the room temperature Hall coefficient, which departing from being determined by the entire Fermi surface complement of quasiparticles above p_c (as in the Narduzzo work [15]), now regresses to track only the number of 'holes' away from $^9Cu^0_{II}$ [5]. In the extreme stripe model the holes reside solely on the stripes, the rivers of charge [10]. The pseudogapping records this rapid decline in the number of active quasiparticles. Within the domains between the stripes the Cu sites there all evolve steadily towards a frozen $^9Cu^0_{II}$ Mott aspect. Such changes have a marked effect upon the p dependence of the chemical potential, it transferring from band-like accommodation to p (i.e. to the average Cu valence)

above p_c to becoming pinned in energy below p_c, as with a doped semiconductor. This crossover in behaviour can readily be followed by core-level photoemission [40]. In LSCO, where striping is developing strongly, the transformation is very clear cut (see figure 3 in [40]). Note the states for which the strongest changes in core line position are manifest are the Sr and La 3d states, the ones most directly interactive with and responsive to any modification to Cu 3d conduction band character. The loss of spectral weight from the band-like cohort of states, which loss of coherence and the pseudogapped condition entails, has recently been pursued also through analysis of the electronic Raman spectra [41] and the ARPES spectra [42] by Storey *et al* and Sahrakorpi *et al* respectively. One does not have to believe in Fermi arcs *per se*, but simply that persistence of the chronic scattering impels a broadening of their *complementary* states into incoherence; namely the states of the FS saddles most active in the negative-U boson/fermion crossover events.

An additional observation relating to Hall work might be dealt with here before turning finally to the purported matter of quantum oscillations in underdoped HTSC material. This concerns the recent high field (50–65 T) data from Balakirev *et al* [43] and their uncovering just below $p = p_c$ of *non*-monotonic behaviour in $R_H(p)$ at low T. The new work uses high quality thin-film samples of LSCO and is a follow-up study to comparable work on $Bi_2(Sr_{2-x}La_x)CuO_{6+\delta}$ in 2003. When the authors make to convert their $R_H(T, p)$ findings into an effective Hall number $n_H(T, p)$ via a simple inversion it could seem that the non-monotonic behaviour at low temperature amounts to a temporary recovery in active quasiparticle numbers after the initial fall at p_c. This recovery would peak narrowly a little above p^{opt}, before ultimately n_H drops away steeply again. In [43] there follows once more an appeal to QCP for explanation of this perceived behaviour. However one has to remember that the established anisotropy in $\ell(\mathbf{k}_F)$ renders simple inversion of R_H to obtain n_H invalid. It is my understanding that what is being observed here arises from the rapid improvement in the *average* mean free path following the elimination from play of the antinodal quasiparticles. It was revealed several years ago now by Krishana *et al* [44] from thermal conductance work that in a magnetic field the electronic contribution to κ_{th} is increasing rapidly down through T_c. The present Hall experiment, wherein T_c is quenched, would indicate this rise to be reliant not on precursor superconductivity but on the changes to the 'normal' state electronic *scattering* coming for such p sitting slightly below p_c.

4. An end to Fermi liquid quantum oscillations in underdoped HTSC material

There is no problem with seeing quantum oscillations as set by the large Fermi surface present in strongly overdoped HTSC material, provided one is able to go to sufficiently high magnetic fields ($> H_{irrev}$). dHvA and SdH studies on strong coupling superconductors have become routine since the ground breaking work on 2H-$NbSe_2$ [45], even though H might stand below H_{c2}. Very recently Vignolle *et al* [17] have managed to secure both magneto-resistance and magnetic torque oscillations from small, high quality (RRR $\sim$ 20), highly overdoped Tl-2201 crystals, with $T_c \approx 10$ K, by working at sub-4.2 K temperatures and in fields of between 50 and 60 T (here $> H_{c2}$). The single observed Fourier frequency of 18 100 T corresponds to a hole FS occupying 65% of the area of the Brillouin zone, i.e. to a 'p value' (reckoned from half-filling) of 0.30. That outcome is totally in accord with band structure calculation [46], with ARPES data [47], with the angle-dependent magneto-resistance data [16], and of course with the T_c value [48]. No problem here then, but there occurs one alerting feature emerging from the data, namely the quasiparticle effective mass. Here at $4.1m_e$, m^* is already very considerably greater than the calculated band mass of $1.2\ m_e$, whilst the mean free path even in this highly overdoped material is only ~500 Å—and yet we still have to encounter the vast bulk of the correlated behaviour to come as the value of p is reduced.

One should not contemplate then results in any way comparable to the above coming from optimally and especially underdoped material. People for many years have endeavoured to obtain dHvA/SdH oscillations from optimally doped Y-123, Bi-2212, etc, including operating to much higher pulsed fields, but without any sign of success. So how could it be that several groups have over the past $2\frac{1}{2}$ years detected what appear to be very like quantum oscillations issuing from—all the more remarkably—material which is significantly underdoped, namely $YBa_2Cu_3O_{6.5}$ [18c] and $YBa_2Cu_4O_8$ [18b], wherein, as we saw earlier, the chronic scattering has brought the Fermi liquid into incoherence? Clearly the answer to this riddle has to lie with the fact that these experiments on the underdoped material turn up a single frequency some 30 times smaller than what is seen with OD-Tl-2201. This would amount to an area in k-space of only about 2% of the Brillouin zone, and without registry occurring of any larger piece. To those inured in metal physics the overwhelming temptation, at this point, has been to turn to some density-wave reconstruction of the original Fermi surface, driven either by charge, or spin, or stripe superlattices, or whatever. After all one has the ARPES 'Fermi arcs' to conjure with. Accordingly we have seen a whole series of band-folding scenarios pass by. These invariably have however in one way or another lost sight of the true experimental circumstance one meets with in the pseudogap regime of underdoped HTSC systems. Take as an example the 1D stripe scenario developed by Millis and Norman [49]. Because the Doiron-Leyraud work [18c] on oscillations in R_H pointed out that the Hall coefficients are negative in these UD materials under the given conditions, some negatively signed bit of folded FS of appropriate area must necessarily dominate the source of the experimental signals. But where does the ascribed negative bit of FS derive from? It would issue from the high mass, saddle region of the parent band structure, precisely where the chronic scattering was destroying quasiparticle coherence. In conflict with this prescription note that, while showing the anticipated size and sign, this said bit of 'FS', as it is assessed via the quantum oscillation analysis, would manifest an effective mass that at $2m_e$ is only half that found for highly OD Tl-2201 [17] where the correlation had barely begun to be injected. Each of the proposed scenarios contains some equally suspect feature; however I do not at

this point wish to pursue them all individually. Let us break away to consider an avenue of interpretation that is quite different, one dependent upon the most mobile electrons, not the least. Moreover it is not a k-space-based argument, but a real space argument, one centred upon the diagonal 'rivers of charge' of the 2D-striped environment which earlier I have presented as characterizing the underdoped systems [10, 11]. This course will provide an altogether more local and robust way of matching the observations than can ever be obtained in the current circumstances from a k-sensitive density-wave recasting of the Fermi surface geometry.

The fields employed in the new experiments (on underdoped material) of around 50 T are greater than $H_{\rm irr}$ though still here below 'H_{c2}', especially as extended up into the Nernst region in underdoped material [50]. Thus we are in the region in which the fluxons are not strongly pinned but will distribute much more uniformly. With magnetic fields ∼10 G we were able directly to observe in Bitter decoration experiments the fluxon arrays there take up regular spacing S of around 1.5 μm [51]. Now with fields 5×10^4 times larger one will, with $B \propto 1/S^2$, be looking at fluxon spacings some 2×10^2 times smaller, namely $S \sim 7$ nm. At $p = \frac{1}{8}$ the 2D stripe domain has edge $D = (8/\sqrt{2}) \times 4$ Å, i.e. 22 Å or 2.2 nm [10]. Accordingly, with the above fluxon spacing (≈3.2 domain lengths), around 1 domain in 10 will contain a fluxon core. Note such a fluxon commensuration number m ($\equiv S^2/D^2$) holds direct resonance with the observed 'order' of the oscillation peaks stationed in the dHvA traces near 50 T. The 'fundamental' field ($m = 1$), under application of *reciprocal* extrapolation, then comes to stand at around 500 T [18]. This is quite a small value for dHvA work, it being equivalent as noted above to ∼2% of the BZ.

Before looking more closely at the numbers we first must consider the basics of what appears to be unfolding here. It would seem that, analogous to the set Fermi surface cross-sectional area within k-space of the conventional dHvA ascription, one here has in real space a fixed, p-determined, array of stripe domain boundaries, and past these, as the magnetic field is ramped up and down, progressively transfer the fluxons. Recall the fluxon core size is controlled by the coherence length, and for HTSC materials it may be as small as 15 Å, i.e. below the relevant domain sizes here. It is not unreasonable then to assume that fluxons will prefer to sit centrally within a domain, i.e. integrally, so that one witnesses successive magnetic free energy turning points as the fluxon number density is made to transit through, for example, the numerical commensurations 12 fluxons per 12 domain span, 11 per 11 domain span, 10 per 10, and so on, as H is ramped up. In this process the area allotted to each fluxon enlarges per 'click' by a single diagonal stripe domain. One can anticipate many derivative properties such as the magnetization and the transverse Hall coefficient then to oscillate in step with the adjusting domain number counts per fluxon. Besides the magnetic aspect remember we remain below H_{c2} and that at low temperatures induced supercurrents will flow around the metallic stripe boundaries, where the local pairs are stable. Hence one may expect the bulk resistivity will oscillate too, even if one resides only in the Nernst region. Real space dictated oscillations not too dissimilar to the above have been recorded from the metallic edge states of quantum dot arrays constructed from materials that in the bulk state are semiconductors [52]. Considering the preceding scheme to be of potential merit, we shall below make a more detailed examination of the actual experimental data to see if it is possible to confirm this story-line.

First it is appropriate to point out some severe difficulties are in fact posed by the current data towards any *standard* quantum oscillation interpretation, even were one to presume the metal examined to be quite conventional. Notably with neither Y-124 nor $YBCO_{6.5}$ do the measured fundamental 'dHvA/SdH' frequencies and associated k-space areas express compatibility with Luttinger's theorem, should the above measured pocket prove the sole *type* of pocket to exist. If just one such pocket per zone were present, then it would be too small, whilst with four such pockets, it would be too large to match the number of p-type carriers that stoichiometry and the customary hole-type treatment of UD HTSC materials dictate; namely $p = 0.11$ in the Y-124 case and $p = 0.10$ for $YBCO_{6.5}$. If by contrast there were to be electron pockets in addition to hole pockets, as could happen with a Fermi surface reconstruction event, then new problems arise in relation to the specific heat [8]. The electronic specific heat implicit in such a case would automatically become greater than the observed value [18d], unless some carriers were to go unregistered through localization. Actually the Hall coefficient observed at low temperatures and high fields (namely 30 $\rm mm^3\ C^{-1}$) provides a rather close match in magnitude for just a *single* pocket of the indicated size [18d]. The most striking fact, though, as pointed out earlier, is that the Hall sign has under the experimental conditions crossed over into becoming *negative*. It was this latter observation which when one resorts to a more complex Fermi surface reconstruction scenario leads to problems over the sourcing of a piece of FS of such high mobility it is able to dominate both the Hall and the SdH/dHvA responses. There is one strong indication, however, that this negative sign to $R_{\rm H}$ at low T in underdoped material comes not from Fermi surface governed density-wave formation but from stripe formation within the current, inhomogeneous, mixed-valence chemistry. This is provided by the observation that even in low fields for LBCO($p = \frac{1}{8}$) a comparable swing in sign of $R_{\rm H}$ is closely coupled there with the LTO-to-LTT structural phase transition [18d, 10]. Now diffraction measurements, whether by neutrons or electrons, have established that stripe order becomes so strong in the latter material as to freeze quasi-statically, restraining $T_{\rm c}$ there to uniquely low values. It by association would appear that the negative response Hall developed in Y-124 and $YBCO_{6.5}$ comes as the strong applied magnetic field strengthens their striping tendency. From the inelastic neutron work of Lake *et al* on LSCO [53] it is known that a magnetic field drives up the l.t. magnetic spin gap aspect to the domain interiors, thereby increasing differentiation of the latter from the domain boundaries, the rivers of charge. The stripe carriers no longer are controlled in their response to a magnetic field by the Fermi geometry, they simply are electrons and behave classically. This ought in truth to come as a relief to Fermiologists since the

Table 1. Model values (see text) for oscillatory repeat features to be expected with 'striping' superlattices of $8a_o$, $9a_0$ and $10a_o$ due to interaction with vortex array. In the modelling of [10, 11] the 'striping' is in fact two-dimensional with the stripes or 'rivers of charge' running in the diagonal directions.

• For $p = 1/8$: supercell edge $= 8a_o$
Average basal lattice const. $a_o = 0.3855$ nm.
$\therefore$ diagonal domain edge $8a_o/\sqrt{2} = 2.1810$ nm $(=D)$,
and diagonal domain area $= 4.7568$ nm$^2(=D^2)$.
For 'fundamental' oscillation appropriate to applied field B_1 require fluxon number density, in units of domain area D^2, to equal *unity*, i.e. $B_1 D^2/\Phi_o = 1$.
Taking as Φ_o, the flux quantum, $h/2e = 2.067 \times 10^{-15}$ Wb or 2067 T nm^2, here $B_1(=\Phi_o/D^2) = 2067/4.7568 = 434.5$ T, —with $B_m = B_1/m$.

• For the case appropriate to $p = 1/9$, where dealing with domain of edge $9a_o/\sqrt{2}$, scale by $(8/9)^2$ to get $B_1 = 343.3$ T.
(or $B_{(1)} = 686.2$ T, see text).

• For case appropriate to $p = 1/10$, where dealing with domain of edge $10a_o/\sqrt{2}$, scale by $(8/10)^2$ to get $B_1 = 278.1$ T. (or $B_{(1)} = 556.2$ T, see text).

• Y-123$_y$, $a_{\rm av}$, see figure 6 in [67]; Y-124, $a_o = 0.3841$ nm, $b_o = 0.3871$ nm.

Dom. edge Calc$^{\rm d}$. order m	$8a_o/\sqrt{2}$		$9a_o/\sqrt{2}$		$10a_o/\sqrt{2}$		Data order	
	B_m (T)	$1/B_m$	B_m (T)	$1/B_m$	B_m (T)	$1/B_m$	$m^{\rm exp}$	
	869.0	*0.001 15*	*686.2*	*0.001 46*	*556.2*	*0.001 80*	(1)	$\frac{1}{2}$
1	434.5	0.002 30	343.1	0.002 91	278.1	0.003 59	(2)	1
	—		*228.7*	*0.004 37*	*185.4*	*0.005 39*	(3)	$1\frac{1}{2}$
2	217.3	0.00460	171.5	0.005 83	139.0	0.007 19	(4)	2
	—		*137.2*	*0.007 29*	*111.2*	*0.008 99*	(5)	$2\frac{1}{2}$
3	144.8	0.006 90	114.4	0.008 74	92.7	0.010 78	(6)	3
	—		*98.0*	*0.010 20*	*79.5*	*0.012 56*	(7)	$3\frac{1}{2}$
4	108.6	0.009 21	85.7	0.011 66	69.5	0.014 38	(8)	4
	—		*76.2*	*0.013 11*	*61.8*	*0.016 18*	(9)	$4\frac{1}{2}$
5	86.9	0.011 51	68.6	0.014 57	55.6	0.017 98	(10)	5
	—		*62.4*	*0.016 03*	*50.6*	*0.019 78*	(11)	$5\frac{1}{2}$
6	72.4	0.013 81	57.2	0.017 49	46.4	0.021 57	(12)	6
	—		*52.8*	*0.018 94*	*42.8*	*0.023 37*	(13)	$6\frac{1}{2}$
7	62.1	0.016 11	49.0	0.020 40	39.7	0.025 17	(14)	7
	—		*45.7*	*0.021 86*	*37.1*	*0.026 97*	(15)	$7\frac{1}{2}$
8	54.3	0.018 41	42.9	0.023 32	34.8	0.028 77	(16)	8
	—		*40.4*	*0.024 77*	*32.7*	*0.030 56*	(17)	$8\frac{1}{2}$
9	48.3	0.020 71	38.1	0.026 23	30.9	0.032 34	(18)	9
	—		*36.1*	*0.027 69*	*29.3*	*0.034 16*	(19)	$9\frac{1}{2}$
10	43.5	0.023 01	34.3	0.029 15	27.8	0.035 96	(20)	10
Re	—		$YBa_2Cu_4O_8$ $p = 0.111$		$YBa_2Cu_3O_{6.5}$ $p = 0.100$			

Fermi surfaces of Y-123 and Y-124 are significantly different in their form and number of bands, and thus why should the oscillation data they supply emerge so alike? As the data are independent of basal field direction they have without doubt to be associated with the planes, but one final feature affirms that Fermiolgy is not the answer here; the new data support no c-axis dispersion whatsoever, in spite of the smallness of the claimed pockets. They exhibit the $\sec\theta$ tilt behaviour of strict two-dimensionality.

Let us see now then just how closely the real space model might be able to provide a match to the UD oscillation data. We shall start with a straightforward case based on $p = \frac{1}{8}$, the individual domains here being of edge $D = 8/\sqrt{2}a_o$, the latter set diagonally within a square supercell of side $8a_o$ [10, 11]. For the fundamental oscillation, appropriate to applied field B_1, we request that the fluxon density, in units of the domain area D^2, be equal to unity; i.e. $B_1 D^2/\Phi_o = 1$: this yields $B_1 = 434$ T. In a reduced field B_m, for which m vortices in the diluted vortex lattice now occur distributed over an area $(mD)^2$ (with a stripe crossing-point defining the real space origin), the associated field B_m will be down on B_1 by the factor $1/m$; i.e. at these geometric coincidences $B_m \propto 1/m$. These 'high order' fields B_m and their reciprocals $1/B_m$ are evaluated in the leading section of table 1 for the first ten cycles in sequence m. They relate to allowing this running number m of fluxons in the vortex superarray, within linear dimension mD, integrally to ratchet up as the field strength declines down through the listed B_m. While these calculated 'data points' are in the general region occupied by the actual oscillatory data, the gradient of the plot secured in figure 2 is clearly too steep. What is more there appear to be something like twice as many experimental oscillations as are being calculated here. Now the above calculation was not of course made for the actual doping level either for Y-124 or $YBCO_{6.5}$. Consider first the 123 material over which there is less argument as to what the correct p value might be. With a T_c of 57 K the $YBCO_{6.5}$ sample clearly is appreciably below the T_c plateau imposed upon the Y-123 $T_c(p)$ plot by the special doping value of

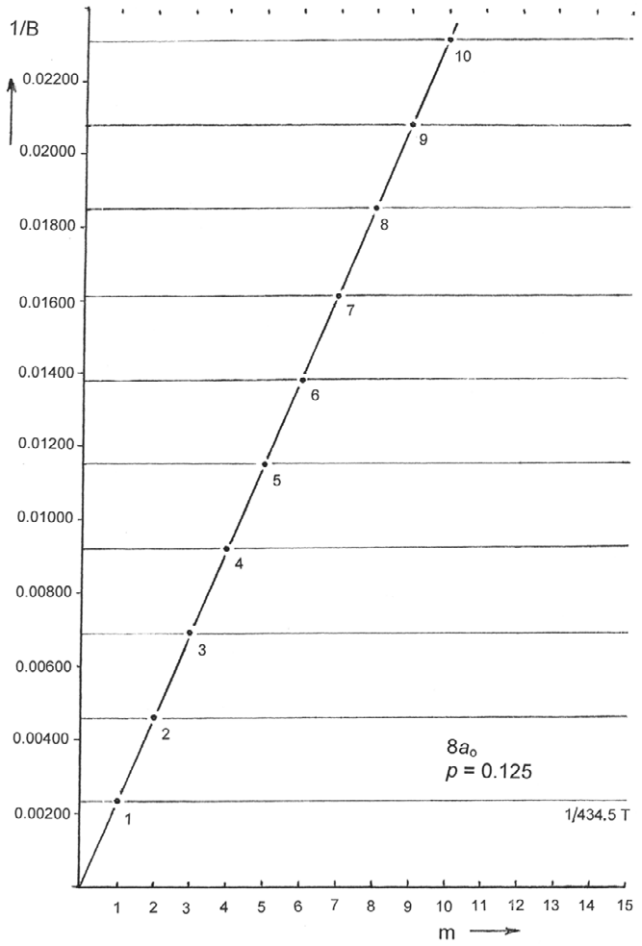

Figure 2. The set of calculated values of $1/B_m$ versus integers $m(=S^2/D^2)$ for case of $p = 1/8$ and square superlattice $8a_o$. Following the 'stripe ' modelling of [10] the stripes themselves are diagonal in orientation and define here domains of edge $8a_o/\sqrt{2}$. Note as $S^2 = mD^2$, $m(S^2) = (mD)^2$; i.e. m fluxons will thread a square set of m^2 stripe domains. The fundamental field $B_1 = 434$ T.

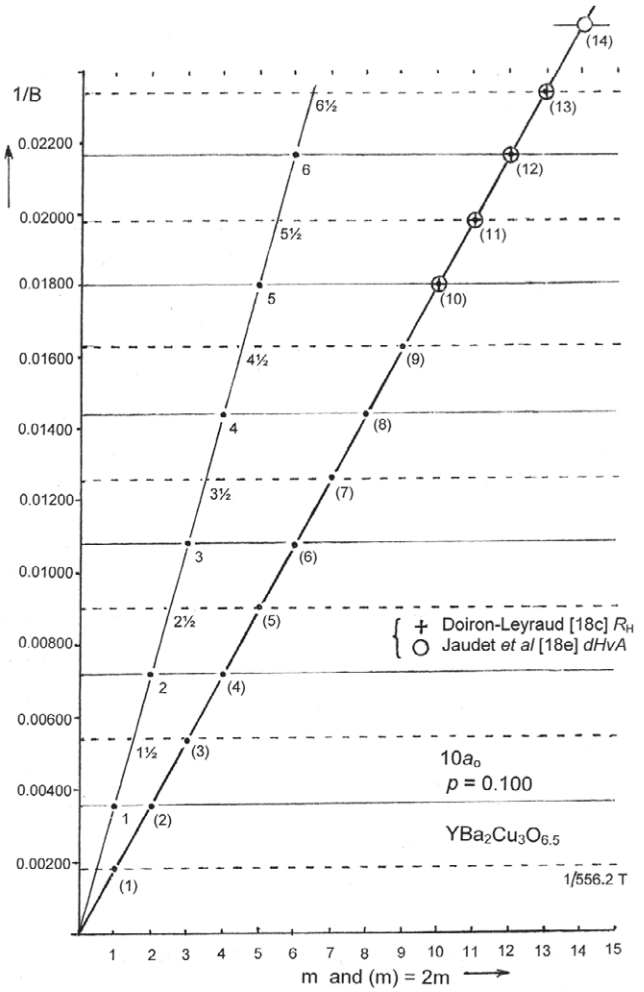

Figure 3. Reworking of figure 2 for $p = 1/10$ and striping superlattice period of $10a_o$, appropriate to case of $YBCO_{6.5}$. The crosses and circles relate to the data cycles recorded by Doiron-Leyraud *et al* [18c; R_H] and Jaudet *et al* [18e; τ]. There are twice as many oscillations, (m), as were first expected, m, (see text), but the match of the calculated $B_{(m)}$ values to the full-integer and half-integer data set is excellent. The fundamental value of $1/B_{(1)}$ inverts to a field of 556 T.

$p = \frac{1}{8}$. There exists in fact general consensus that a value of $p = 0.100$ is appropriate for $YBCO_{6.5}$ (see 'methods' in [18c]), and the above fields B_m accordingly will need to be rescaled by $(\frac{8}{10})^2$ in order to relate to the associated $10a_o$ supercell (see table 1, section 3). This automatically is going to lead to a $1/B_m$ versus m plot which however is even steeper now than it was for $p = \frac{1}{8}$ (one is required to look to reduced m to accommodate the new $1/B_m$ set). Quickly though it is noticed that the new intervals in $1/B_m$ do now follow the experimental data precisely *were one* to consider half-intervals also (defined by half-integer values of m). Figure 3 shows the situation for $p = \frac{1}{10}$, where we make comparison to the $YBCO_{6.5}$ dHvA data set secured by Jaudet *et al* [18e]. The longest continuous trace which they present is their figure 3, reproduced now in the appendix with added markers. There we find that actually it is points regularly phase-shifted from the *minima* in the magnetic torque trace which perfectly match the $10a_o$ $\frac{1}{2}$-integer prescription. The oscillations from left to right in figure 3 of [18e] extend from (10) to (17), these running numbers being now quoted in brackets to designate that they here refer to half-integer sequencing, i.e. to $2m$. The same association holds good for the more limited set of dHvA magnetization results given by Sebastian *et al* [18f] in their figure 4.

Two questions arise: why do half-integers seem to feature here, and why does the sequencing require counting back not always on the peaks of the various experimental signals but often elsewhere within the cycle, to reveal the 'fundamental' field equal above to 556 T? Before these questions are answered it is best to examine how the situation unfolds for Y-124.

As stated there is some dispute as to what the appropriate value of p actually is for $YBa_2Cu_4O_8$. I much disagree with the value of 0.14 adopted by LeBoeuf *et al* [18d] and Bangura *et al* [18b], and favour a considerably lower value, in fact somewhat lower than 0.125. This opinion is based on two counts. In $YBa_2Cu_3O_7$ the maximal T_c of 92 K arises in material for which $p \approx 0.16$. There, with its stoichiometry dictated *average* Cu valence of $2\frac{1}{3}$, one third of a hole in total

has to pass to the chain Cu site to leave behind just $\frac{1}{6}$ of a 'hole' (re d^9) per planar Cu site. In $YBa_2Cu_4O_8$, with an average Cu valence now of only $2\frac{1}{4}$, an analogous transfer of one quarter of a hole passing in total to the two chain Cu's would leave behind just $\frac{1}{8}$ of a hole on each planar Cu site. But the hole transfer to the chains is likely in fact to be a little greater since the electronegativity difference between the planes and chains is still substantial. Thus a residual planar 'hole' count of $p = \frac{1}{9}$ seems not unreasonable. Recall that an appreciable underdoping for Y-124 is indeed signalled by its very large T_c pressure coefficient [54], T_c readily being pushed up from 80 to 108 K. Such pressure coefficients arise only with significantly underdoped material (as for $YBCO_{6.5}$). Y-124 is considered then as being stationed somewhat below the T_c plateauing associated with $p = \frac{1}{8}$ in Y-123, etc. Accordingly in table 1 section 2 one will find the comparable values for B_m and $1/B_m$ relating to a $9a_o$ stripe superlattice. Possibly here the action of the strong applied magnetic field is to impose such commensurate structure upon Y-124: LeBoeuf *et al* indeed report a sharp discontinuity in R_H at 40 T [18d, figure 3c]. Once again it soon becomes apparent that these evaluated reciprocal fields $1/B_m$ in section 2 of the table match the 124 data (e.g. figure 2 in [18b]) rather closely, but only after being required to make the above half-integer accommodation, as is in evidence from figure 4. The fundamental field $B_{(1)}$ this time emerges from the domain model as being 686 T, as against 556 T with $p = \frac{1}{10}$ $YBCO_{6.5}$. The experimentally adduced values for $B_{(1)}$ were (over optimistically) quoted as 660 ± 15 T [18b] and 540 ± 4 T [18e] respectively. Our calculated $1/B_m$ repeat *separations* match the data even better (see appendix). The field and temperature dependencies of the oscillatory signal *amplitudes* are ascribable to the level of long range order attainable in the vortex array. Under the experimental conditions one is just emerging from the pinned vortex regime around 40 T.

So now how might we view the above half-integer behaviour with regard to the basal areas responsible for generating the oscillatory field traces. One straightforward interpretation would be that it represents a projection effect from an ABAB two-sheet stacking sequence of the charged domain boundaries, their displacement directed at 45° to the *b*-axis orientation of the chains. The threading of the fluxons through the sample as a whole then will be expressed by cross-sectional areas just half of what they would be were the domains and their boundaries directly to superpose between successive sheets. Note that, simple though it may be, I do not in fact advocate this solution. It relates to current circuits divided between sheets from which there is not going to be ready charge transfer, with serious impact upon mean free path maintenance of the appropriate level. Moreover it breaks symmetry as we shift to area-defining oblongs, and the 45° orientation of the stacks inevitably would lead to a chaotic jumble of twins. Now from low temperature, small angle neutron diffraction scattering (SANS) studies on the best bulk samples it is known that the orientational characteristics of the vortex array are fairly stable. Even more significantly it is well established that at higher fields the diffraction spotting reveals the fluxon array to undergo transfer from being hexagonal to

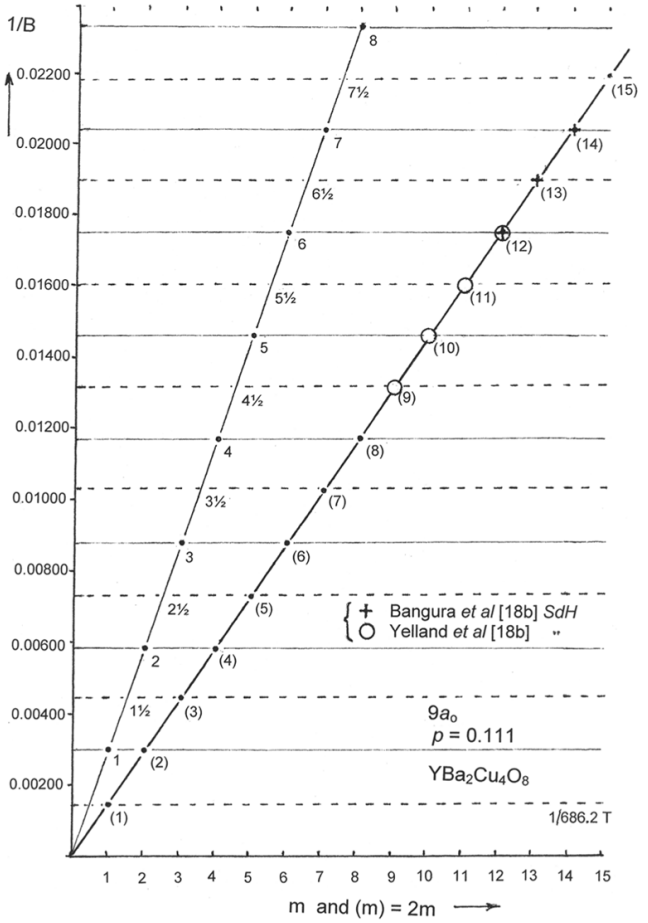

Figure 4. Similar plot to that of figure 3 but now for p value of 1/9 and striping superlattice period $9a_o$, appropriate to case of $YBa_2Cu_4O_8$. The crosses and circles relate to the data cycles recorded by Bangura *et al* [18b; $\Delta\rho/\rho$] and Yelland *et al* [18b; inductance]. Here fundamental value for $1/B_{(1)}$ of 0.001 46 inverts to a field $B_{(1)} = 686$ T.

becoming square [55]. I have taken this fact to signal the fluxon locations become constrained to the striping geometry. The authors of the SANS work presumed the striping was 1D, and thus they were not drawn to such a line of interpretation. At the time of their finding in 2002, my own view of 2D striping was that the orientation of the square domains was axial [56], and hence I did not perceive at that point that, due to the LSCO LTO $\sqrt{2}a$ structuring, the reported orientation of the square array of SANS spots in [55] was in fact 'diagonal': precisely as would come to match my revised appreciation of the stripe domain geometry made in 2005 [10]. Such accommodation of the fluxon array to the striping is not the only feature of relevance here. In addition to the square order emerging at raised fields (>0.8 T), the material in which it arises is underdoped, or at least in the case of Gilardi's paper for LSCO $p = 0.17$ [55] having a p value below p_c. These are just the conditions under which low temperature striping becomes best organized, and accordingly most constraining upon the geometry of the traversing fluxon array. There is in figure 2 of [55] no indication, note, of any array twinning, even with the LTO structure.

Given these circumstances, if we are not to favour a layer stacking sequence origin to account for the appearance of the half-integers implicit in the present oscillation work, what might be the alternative? The point in the stacking proposal was to attain a fixed set m of fluxon-encompassing, stripe-bordered regions twice as numerous as had been anticipated. But the same effect may of course be secured, not by halving the incremental areas, but by doubling the relevant flux quantum. If the imposed flux density is divided into quanta of h/e rather than $h/2e$, all the fields B_m will then need doubling to gain any desired fluxon running number, so shedding the perplexing half-integers, just as is manifest on figures 3 and 4. This suggestion has the advantage of being very 'clean' and of leaving the rivers of charge directly superposed between successive sheets. It is a solution that one might regard as not entirely unheralded, given the fact that we are dealing with a local pair superconductor and with an array of strongly anisotropic vortices tightly set about by the stripe boundaries. We already have the precedent of abnormal fluxons in the beautiful manufactured boundary experiments of Tsuei *et al* [57] which served to confirm the effectively d-wave nodal character of the HTSC superconductors. In the presently considered geometry we see the diagonal 2D striping array is set at an angle of 45° to the axial direction and accordingly runs in the nodal direction of the superconductivity.

How might one now cope with the second query above regarding the observation (evident in the data sets reproduced in the appendix) that the model does not uniformly relate to one common feature between the various different oscillatory traces; say the peaks, the troughs, etc. This variety of observed phase shifts necessarily must reflect not only the different forms of experimental routine actually pursued, but also the physical character of the stripe domain interior—and in particular with dHvA how it relates to magnetism. In my analysis of the latter condition, upon appeal to the magnetic circular dichroism results of Kaminski *et al* [58], I in [11] emerged with the in-plane circulatory spin patterning within the domains displayed there in figure 2(b). Such an outcome has duly acquired support since from Fine [59] through his direct analysis of the neutron diffraction data, from Di Matteo and Norman [60] via their analysis of the x-ray circular dichroism data, and from Shi *et al* [61] following further infra-red Hall, Faraday rotation and circular dichroism experimentation. It is envisaged that well within the domains the spins are settling into spin-gapped, RVB-type singlet coupling [53], but that close to the domain periphery the spins become canted, conforming to the bounding stripes under the magnetostrictive effects of the lattice, arising there under valence segregation and the Jahn–Teller effect. These canted spins are viewed as responsible for the weakly magnetic conditions now reported on by Fauqué *et al* [62] and by Li *et al* [63] for underdoped YBCO and HgBCO respectively: the moments here, upon being averaged per Cu site, amount to only $\sim 0.1\ \mu_{\mathrm{B}}$.

We are finally in a position now to consider how we are to 'reference' the matter of phasing. In the customary Lifshitz–Kosevich formulation of the oscillatory magnetization the form used is $\sin(2\pi F/B + \phi)$. In these terms the traces appearing in the appendix for $\Delta\rho/\rho$ from Bangura *et al* [18b], for the inductance signal from Yelland *et al* [18b], for the oscillatory torque data from Jaudet *et al* [18e], and for $-\Delta R_{\mathrm{H}}$ from Doiron-Leyraud *et al* [18c] are respectively of phasing $\phi = 0, \pi/2, \pi$ and $-\pi/2$. A second detail of phasing assignation is how to seat the stripe superlattice itself relative to the real space origin: does one select a stripe or a domain centre to be so placed? The simplest choice would be the former since we have used the stripes themselves for counting purposes. But does that choice mesh in meaningfully then with the experimental observations? It would seem so. Δf in Yelland *et al*'s experiment is $\propto \mathrm{d}M/\mathrm{d}B$, making M itself maximal at $\phi = \pi/2$, where the flux vortex will sit central to the domain and the magnetic $^{9}\mathrm{Cu}_{\mathrm{II}}^{0}$ sites then will be maximally in play. The Jaudet *et al*'s torque phasing of π issues from $\tau = -(\Delta\mathbf{M}) \times \mathbf{B}$ in the presence of antiferromagnetic coupling. Maxima in $|\Delta\rho|$ (or rather minima in longitudinal mobility) are to be expected under a phasing for which each flux line coincides with a transverse stripe, supplying $\phi = 0$ for Bangura *et al*'s trace. The $\phi = -\pi/2$ phasing applicable in Doiron-Leyraud *et al*'s trace is because they track $-\Delta R_{\mathrm{Hall}} \propto -\Delta p$, the effective change in content of responding holes in underdoped material. It would appear then that the choice made above was the appropriate one, and that these various differences in trace phasing are capable too of being satisfactorily embraced within the proposed stripe domain/vortex array modelling.

The actual cyclical profile of the experimental oscillatory signal is finally, one might observe, neither decaying monotonically, as Yelland *et al* pointed out in [18b], nor is it of simple harmonic form. There looks to be a tendency towards a more complex oscillation profile, perhaps of saw-tooth character. The analysis made by Sebastian *et al* [18g] would appear to support this upon reading their third Fourier peak to in fact be the third harmonic. One sees it to be considerably stronger than the second harmonic. Unfortunately Sebastian *et al* have interpreted their third peak as evidence of an independent orbit, the outcome of them being unable to specify their fundamental closely enough as a result of the short field span which their experiment covers.

In closing this section I append a more formal statement of the law of dilution of the vortex array as H falls which has been employed above.

- Take a square superarray of vortices, side mD, and let m vortices fall in this area.
- Let the system *dilute* to $(m+1)$ vortices now set in square superarray of side $(m+1)$ linear units, D, or $(m+1)^2$ areal units, D^2.
- The incremental area here is $2m+1$, i.e. $m + (m+1)$.
- Each of original m vortices has increased its areal footprint by 1 (stripe domain) to $(m+1)$, and in addition we have embraced the extra vortex with this same footprint $(m+1)$.
- We thus arrive at our recurrent sequencing of $(m+1)$ vortices in an $(m+1)D$ superarray.

To distribute these vortices uniformly and as widely as possible it would appear the solution is to place just one vortex in each column and one in each row. Figure 5(a) shows the

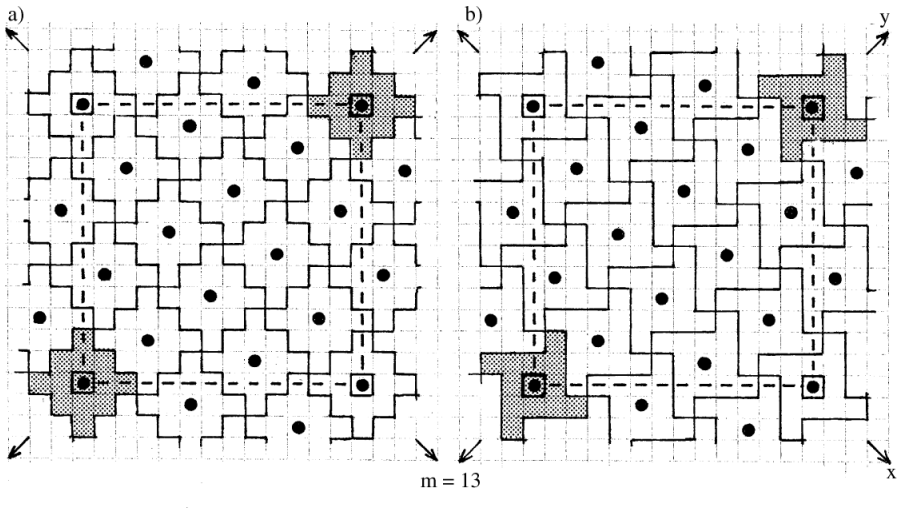

Figure 5. Two vortex tiling solutions for the case $m = 13$. The small squares (side D) are the stripe domains (two-dimensional and in the diagonal/nodal orientation). 13 vortices lie within the square superarray $13D \times 13D$. The vortices in this particular case themselves form a square array of side $\sqrt{13}.D$ in (3, 2) rotation to the nodal direction. Case (a) is of higher tile (i.e. vortex footprint) symmetry than case (b), and so more likely to be adopted. In moving from commensuration $m = 12$ to 13 (to 14), every vortex footprint augments by 1 stripe domain during the dilution step. For all comparable tilings the most compact geometric forms always are to be favoured.

solution for $m = 13$. It is seen that the vortex array itself is square too in this case, but note it is canted relative to the diagonal directions of the stripes, unlike the vortex superarray of side $13D$. Figure 5(b) presents an alternative vortex footprint with $m = 13$, but now this being lower in symmetry is not to be favoured over the form given in figure 5(a). A further paper will present the likely development in footprint form to occur with vortex compaction as H increases. The SANS results of [55b] guide such deliberations below 7 T.

It is hoped that the detailed exposition given above will wean people away from viewing the experimental results from these underdoped HTSC systems as being standard quantum oscillations betokening the existence of a Fermi surface and standard Fermi liquid. That presumption was surely misguided from the start, and it is trusted the present work opens up an altogether more appropriate and potentially exciting scenario to cover the observations.

5. Summary

With section 1 a brief review was provided of the negative-U setting of the boson–fermion crossover scenario for HTSC systems, and of the marked differences existing between the nodal and antinodal conditions. These latter have great implications for the resonance between the local pairs and induced BCS-like Cooper pairs, including how the screening conditions set up at the various doping levels in any given HTSC mixed-valence system afford direct control over the maxima reached in $T_c(p)$.

Section 2 traces in detail the development of the abnormal electrical and optical properties of HTSC systems as 'hole doping' is decreased below $p = 0.3$. For the latter p value the position of the Landau Fermi liquid behaviour is fairly standard if highly correlated. Below $p = 0.3$ there arises a marked growth in scattering and a steady shift towards incoherence. Apportionment of the unusually strong scattering into elastic and inelastic, isotropic and anisotropic contributions is interpreted in terms of e/e-to-b and e-on-b events, after close examination of the T- and p-dependent evolution of the AMRO, Seebeck and Hall data sets.

Section 3 takes a more detailed look at new high quality $\rho(T, p)$ resistivity data and analysis from LSCO, and in particular at the sharp changes coming at $p = p_c(=0.18)$. The nature of what arises there as one meets with strong incoherence and the pseudogap condition is described in terms of the crossover model.

Section 4 follows up on the consequences of such an interpretation and reformulates the setting of the high field oscillatory magnetization, resistivity and Hall data recently obtained from UD material in terms *not* of a standard, quantum oscillation, k-space response of a fairly normal Fermi liquid, but of a real-space-based action much more appropriate to the UD condition. Success here is demonstrated to revolve around the 2D striping supported in such mixed-valence materials and seemingly enhanced in definition in the applied strong magnetic field. The model is one of response to the free energy changes arising as the unpinned vortex array slips discretely through the stripe array. A very close match to the experimental data can be secured *provided* that the flux quantum in question in this ring-threading process is not $h/2e$ but h/e. The observations are related back to Forgan and colleagues' observations on UD material regarding symmetry conversion from hexagonal to square in the vortex array geometry as the magnetic field is increased. Those sceptical of the proffered outcome and requiring theoretical justification of the h/e quantum of flux in question should seek out the paper by Vakaryuk to which my attention has just been drawn in the current issue of PRL [64]. This would appear to relate to just the type of situation described above, though it is not clear how far the fact we are not dealing with point bosons, particularly in the Nernst region above T_c, might be significant here.

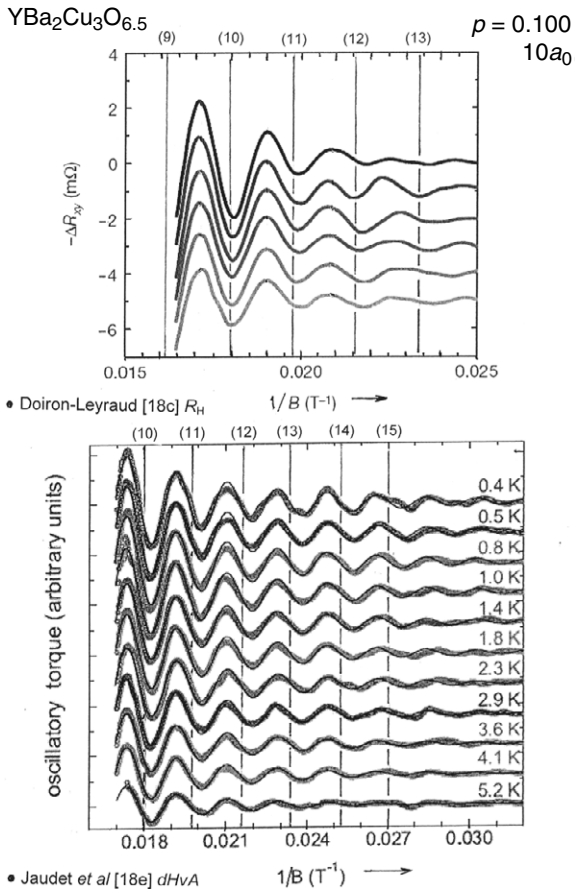

Figure A.1. Modelling from figure 3 superimposed on original data from [18c; figure 3a] and [18e; figure 3a] for $YBa_2Cu_3O_{6.51}$.

Acknowledgments

I would like to thank Nigel Hussey and colleagues for continued discussions on HTSC matters and in particular for advancing to me a copy of their latest work, upon which section 3 is centred, prior to its submission for publication.

Appendix

Indication is made directly on the published data of the level of match for the two underdoped HTSC materials to the oscillation periods secured when employing the present stripe domain/vortex array modelling as opposed to the customary Fermi liquid dictated quantum oscillation interpretation. Figure A.1 is for $YBa_2Cu_3O_{6.51}$, and the data come from Doiron-Leyraud *et al* [18c; figure 3a] and Jaudet *et al* [18e; figure 3a]. The present evaluation takes the hole doping there to be 0.100 supporting a $10a_o$ domain superlattice. Figure A.2 is for $YBa_2Cu_4O_8$, and the data come from Bangura *et al* [18b; figure 2] and Yelland *et al* [18b; figure 2]. The present evaluation takes the hole doping here to be 0.111, supporting a $9a_o$ domain superlattice.

The various phase shifts evident for these data traces are addressed in the text.

The matches presented require one to adopt as flux quantum in the present circumstances a value of h/e rather than $h/2e$, as is highlighted in the text and as very recently broached in the theoretical literature by Vakaryuk [64].

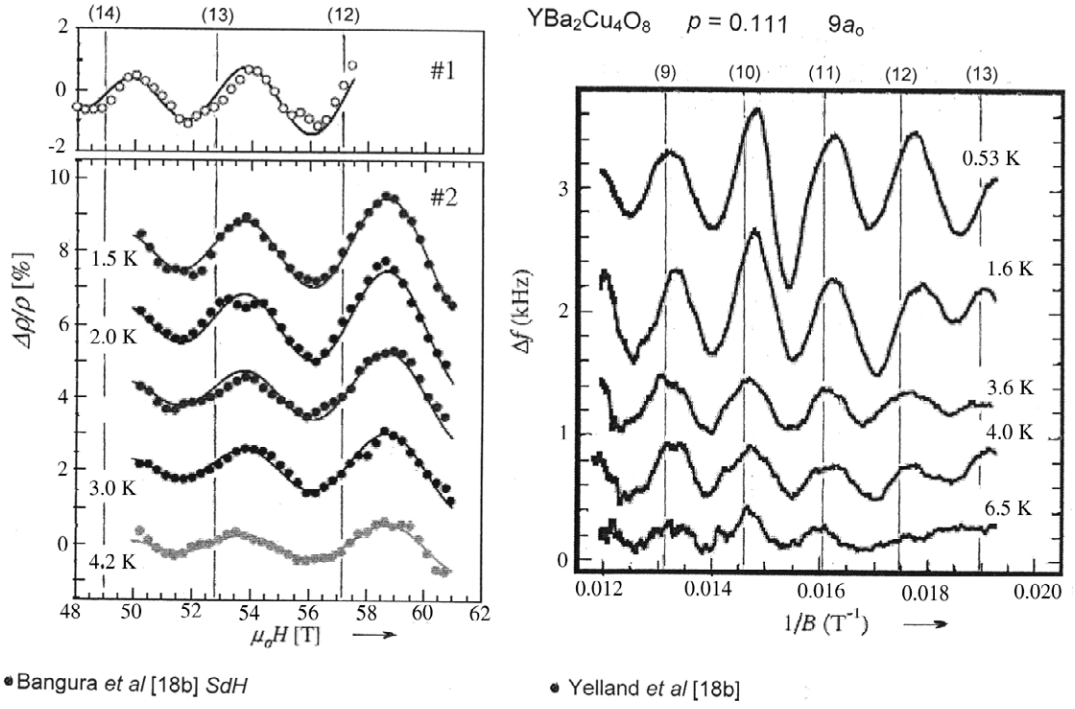

Figure A.2. Modelling results from figure 4 superimposed on original data from [18b; figure 2] and [18b, figure 2] for $YBa_2Cu_4O_8$.

Postscript. I have just received communication from Professor A S Alexandrov that in fact he earlier released a Fast Track paper in April relating these oscillatory observations not to quantized Fermiology, but, as with my own paper, to a real space origin (2008 *J. Phys.: Condens. Matter* **20** 192202). Somehow I had not noticed this work, which, like my own, arises from a disquiet with the Fermi surface controlled interpretation of events and from a conviction that real space pairing is behind HTSC superconductivity. The present scenario is, however, significantly different from that of Professor Alexandrov in that I believe the pairing mechanism to be more electronically based in the negative-U resonant crossover procedure, rather than being the outcome of bipolaron condensation. More specific to the present oscillation problem, I look to the sourcing of the real space periodicity with which the vortex array interacts to come not from the checker-boarding but from the 2D striping (see [10] for distinction).

Finally the reader's attention is drawn to a new release from Audouard, Jaudet and co-workers [66] claiming to supply 3D extension to their earlier dHvA deliberations [18e]. Note that as far as my own interpretation is concerned their two new subsidiary frequencies are those relating simply to a certain amount of $11a_o$ and $9a_o$ stripe superlatticing contaminating the mean $10a_o$ state discussed above: N.B. for the $11a_o$ case, $B_{(1)} = 2 \times (8^2/11^2) \times 434$ T $= 459$ T,—Audouard *et al* extract a $B_{(1)}$ of 453 T. It is remarkable that the stoichiometry in 123-YBCO$_y$ is able to be homogenized even as well as this. In 124, of course, we have a fixed stoichiometry, which above we treated as giving $p = \frac{1}{9}$. The likelihood is that this equivalence is not exact, leading similarly to subsidiary oscillations. Note in the new 123 work [66] that the fraction of the $\sim$140 μm $\times$ 140 μm $\times$ 40 μm sample supporting the $11a_o$ trace ($p = 0.091$) is observed to rise as the empirical overall oxygen stoichiometry drops from $y = 6.54$ to 6.51, as is to be expected with the current modelling. It is essential now to examine the $y = 6.45$ samples known to exist, for which $p \approx \frac{1}{13}$.

References

[1] Wilson J A and Zahrir A 1997 *Rep. Prog. Phys.* **60** 941–1024
[2] Wilson J A 2000 *J. Phys.: Condens. Matter* **12** R517–47
[3a] Wilson J A and Farbod M 2000 *Supercond. Sci. Technol.* **13** 307–22
[3b] Wilson J A 1997 *J. Phys.: Condens. Matter* **9** 6061–8
[4] Obertelli S D, Cooper J R and Tallon J L 1992 *Phys. Rev.* B **46** 14928
[5] Tsukada I and Ono S 2006 *Phys. Rev.* B **74** 134508
Hwang H Y, Batlogg B, Takagi H, Kao H L, Kwo J, Cava R J, Krajewski J J and Peck W F 1994 *Phys. Rev. Lett.* **72** 2636
[6] Kanigel A *et al* 2006 *Nat. Phys.* **2** 447
Kanigel A, Chatterjee U, Randeria M, Norman M R, Souma S, Shi M, Li Z Z, Raffy H and Campuzano J C 2007 *Phys. Rev. Lett.* **99** 157001
[7] Norman M R *et al* 1998 *Nature* **392** 157
Norman M R, Randeria M, Ding H and Campuzano J C 1998 *Phys. Rev.* B **57** 11093(R)
[8] Loram J W, Mirza K A and Cooper J R 1998 *Research Review 1998 HTSC,* ed W Y Liang, IRC, Univ. of Cambridge pp 77–97
Loram J W, Luo J, Cooper J R, Liang W Y and Tallon J L 2001 *J. Phys. Chem. Solids* **62** 59
[9a] Wilson J A 1987 *J. Phys. C: Solid State Phys.* **20** L911–6
Wilson J A 1988 *J. Phys. C: Solid State Phys.* **21** 2067–102
Wilson J A 1994 *Physica* C **233** 332–48
[9b] Wilson J A 2001 *J. Phys.: Condens. Matter* **13** R945
[9c] Wilson J A 2004 *Phil. Mag.* **84** 2183–216
[10] Wilson J A 2006 *J. Phys.: Condens. Matter* **18** R69–99
[11] Wilson J A 2008 *J. Phys.: Condens. Matter* **20** 385210
[12] Kohsaka Y *et al* 2008 *Nature* **454** 1072
[13] Cooper R A *et al* 2009 *Science* **323** 603
[14] Hussey N E, Alexander J C and Cooper R A 2006 *Phys. Rev.* B **74** 214506
[15] Narduzzo A, Albert G, French M M, Mangkorntong N, Nohara M, Takagi H and Hussey N E 2008 *Phys. Rev.* B **77** 220502(R)
[16a] Hussey N E, Abdel-Jawad M, Carrington A, Mackenzie A P and Balicas L 2003 *Nature* **425** 814
[16b] Abdel-Jawad M, Kennett M P, Balicas L, Carrington A, McKenzie A P, McKenzie R H and Hussey N E 2006 *Nat. Phys.* **2** 821
[16c] Abdel-Jawad M, Analytis J G, Carrington A, French M M J, Hussey N E, Balicas L and Charmant J P H 2007 *Phys. Rev. Lett.* **99** 107002
[16d] Analytis J G, Abdel-Jawad M, Balicas L, French M M J and Hussey N E 2007 *Phys. Rev.* B **76** 104523
[17] Vignolle B, Carrington A, Cooper R A, French M M J, Mackenzie A P, Jaudet C, Vignolles D, Proust C and Hussey N E 2008 *Nature* **455** 952
[18a] Carrington A and Yelland E A 2007 *Phys. Rev.* B **76** 140508(R)
[18b] Yelland E A, Singleton J, Mielke C H, Harrison N, Balakirev F F, Dabrowski B and Cooper J R 2008 *Phys. Rev. Lett.* **100** 047003
Bangura A F *et al* 2008 *Phys. Rev. Lett.* **100** 047004
[18c] Doiron-Leraud N, Proust C, LeBoeuf D, Levallois J, Bonnemaison J-B R, Bonn D A, Hardy W N and Taillefer L 2007 *Nature* **447** 565
[18d] LeBoeuf D *et al* 2007 *Nature* **450** 533
[18e] Jaudet C *et al* 2008 *Phys. Rev. Lett.* **100** 187005
[18f] Sebastian S E, Harrison N, Palm E, Murphy T P, Mielke C H, Liang R, Bonn D A, Hardy W N and Lonzarich G G 2008 *Nature* **454** 200
[18g] Harrison N and Sebastian S E 2008 arXiv:0807.3122
[19a] Wilson J A 2000 *J. Phys.: Condens. Matter* **12** 303–10
[19b] Demsar J, Hudej R, Karpinski J, Kabanov V V and Mihailovic D 2001 *Phys. Rev.* B **63** 054519
[20] Bussmann-Holder A and Keller H 2008 *J. Phys.: Conf. Ser.* **108** 012019
[21a] Chung J-H *et al* 2003 *Phys. Rev.* B **67** 014517
[21b] Pintschovius L, Resnik D, Reichardt W, Endoh Y, Hiraka H, Tranquada J M, Uchiyama H, Matsui T and Tajima S 2004 *Phys. Rev.* B **69** 214506
[22] Gedik N, Yang D S, Logvenov G, Bozovic I and Zewail A H 2007 *Science* **316** 425
[23] Röhler J 2004 *J. Supercond.* **17** 159
[24] Saini N L, Oyanagi H and Bianconi A 2004 *J. Supercond.* **17** 103
Bianconi A, Saini N L, Lanzara A, Missori M, Rossetti T, Oyanagi H, Yamaguchi H, Oka K and Ito T 1996 *Phys. Rev. Lett.* **76** 3412
Haskel D, Stern E A, Hinks D G, Mitchell A W and Jorgensen J D 1997 *Phys. Rev.* B **56** R521
Billinge S J L, Bozin E S, Gutmann M and Takagi H 2000 *J. Supercond.* **13** 713
Slezak J A, Lee J, Wang M, McElroy K, Fujita K, Andersen B M, Hirschfeld P J, Eisaki H, Uchida S and Davis J C 2008 *Proc. Natl Acad. Sci. USA* **105** 3203
[25] Varma C M and Abrahams E 2001 *Phys. Rev. Lett.* **86** 4652
Abrahams E and Varma C M 2000 *Proc. Natl Acad. Sci. USA* **97** 5714
[26] Zaanen J 2008 *Nature* **430** 513
[27] Andersen O K, Jepsen O, Liechtenstein A I and Mazin I I 1994 *Phys. Rev.* B **49** 4145
[28a] Tajima S, Fudamoto Y, Kakeshita T, Gorshunov B, Železný V, Kojima K M, Dressel M and Uchida S 2005 *Phys. Rev.* B **71** 094508
[28b] Homes C C, Dordevic S V, Gu G D, Li Q, Valla T and Tranquada J M 2006 *Phys. Rev. Lett.* **96** 257002
[29] Hildebrand G, Hagenaars T J, Hanke W, Grabovski S and Schmalian J 1997 *Phys. Rev.* B **56** R4317
[30] Ong N P 1991 *Phys. Rev.* B **43** 193
[31] Wang Y, Ono S, Onose Y, Gu G, Ando Y, Tokura Y, Uchida S and Ong N P 2003 *Science* **299** 86
Tan S and Levin K 2004 *Phys. Rev.* B **69** 064510
[32a] Hussey N E 2003 *Eur. Phys. J.* B **31** 495
[32b] Hussey N E 2008 *J. Phys.: Condens. Matter* **20** 123201

[33] Allen P B and Mitrovic B 1982 *Solid State Phys.* **37** 2
[34] Houari A and Harris R 1992 *J. Phys.: Condens. Matter* **4** 1505
[35] Chien T R, Wang Z Z and Ong N P 1991 *Phys. Rev. Lett.* **67** 2088
Carrington A, Mackenzie A P, Lin L T and Cooper J R 1992 *Phys. Rev. Lett.* **69** 2855
Manako T and Kubo Y 1994 *Phys. Rev.* B **50** 6402
[36] Koralek J D *et al* 2006 *Phys. Rev. Lett.* **96** 017005
Kordyuk A A *et al* 2004 *Phys. Rev. Lett.* **92** 257006
Kordyuk A A *et al* 2005 arXiv:cond-mat/0508574
[37] Aeppli G, Mason T E, Hayden S M, Mook H A and Kulda I 1997 *Science* **278** 1432
[38] Uemura Y J 2000 *Int. J. Mod. Phys.* B **14** 3703
[39] Rullier-Albenique F, Alloul H, Proust C, Lejay P, Forget A and Colson D 2007 *Phys. Rev. Lett.* **99** 027003
[40] Hashimoto M *et al* 2008 *Phys. Rev.* B **77** 094516
[41] Storey J G, Tallon J L, Williams G V M and Loram J W 2008 *Phys. Rev.* B **78** 140506
[42] Sahrakorpi S *et al* 2008 arXiv:0809.2357
[43] Balakirev F F, Betts J B, Migliori A, Tsukada I, Ando Y and Boebinger G S 2007 arXiv:0710.4612.v1
Balakirev F F, Betts J B, Migliori A, Tsukada I, Ando Y and Boebinger G S 2009 *Phys. Rev. Lett.* **102** 017004
[44] Krishana K, Harris J M and Ong N P 1995 *Phys. Rev. Lett.* **75** 3529
[45] Fletcher J D, Carrington A, Kazakov S M and Karpinski J 2004 *Phys. Rev.* B **70** 144501 and refs therein
[46] Singh D J and Pickett W E 1992 *Physica* C **203** 193
[47] Platé M *et al* 2005 *Phys. Rev. Lett.* **95** 077001
[48] Opagiste C, Triscone G, Couach M, Jondo T K, Jorda J-L, Junod A, Khoder A F and Muller J 1993 *Physica* C **213** 17
[49] Millis A J and Norman M 2007 *Phys. Rev.* B **76** 220503(R)
[50] Wang Y, Lu L, Naughton M J, Gu G D, Uchida S and Ong N P 2005 *Phys. Rev. Lett.* **95** 247002
[51] Sasaki K, Grigorieva I, Bagnall K, Midgley P, Mori T, Wilson J A and Steeds J W 1993 *Japan. J. Appl. Phys.* **32** L990
[52] Räsänen E, Harju A, Puska M J and Nieminen R M 2004 *Phys. Rev.* B **69** 165309
Kato M, Endo A, Katsumoto S and Iye Y 2008 *J. Phys. Soc. Japan* **77** 093715
[53] Lake B *et al* 2005 *Nat. Mater.* **4** 658
[54] Scholtz J J, van Eenige E N, Wijngaarden R J and Griessen R 1992 *Phys. Rev.* B **45** 3077
[55a] Gilardi R *et al* 2002 *Phys. Rev. Lett.* **88** 217003
[55b] White J S *et al* 2008 arXiv:0810.1947
[56] Wilson J A 1998 *J. Phys.: Condens. Matter* **10** 3387
[57] Tsuei C C and Kirtley J R 2000 *Rev. Mod. Phys.* **72** 969
[58] Kaminski A *et al* 2002 *Nature* **416** 610
[59] Fine B V 2007 *Phys. Rev.* B **87** 060504
[60] Di Matteo S and Norman M R 2007 *Phys. Rev.* B **76** 014510
[61] Shi L, Schmadel D, Drew H D, Tsukada I and Ando Y 2005 arXiv:cond-mat/0510794
[62] Fauqué B, Sidis Y, Hinkov V, Pailhès S, Lin S, Chaud X and Bourges P 2006 *Phys. Rev. Lett.* **96** 197001
[63] Li Y, Balédent V, Barišić N, Cho Y, Fauqué B, Sidis Y, Yu G, Zhao Y X, Bourges P and Greven M 2008 *Nature* **455** 372
[64] Vakaryuk V 2008 *Phys. Rev. Lett.* **101** 167002
[65] Alexandrov A S 2008 *J. Phys.: Condens. Matter* **20** 192202
[66] Audouard A, Jaudet C, Vignolles D, Liang R, Bonn D A, Hardy W N, Taillefer L and Proust C 2008 arXiv:0812.0458
[67] Siddique R K 1994 *Physica* C **228** 365